IOP Publishing Physica Scripta
Phys. Scr. 95 (2020) 025205 (14pp) https://doi.org/10.1088/1402-4896/ab43ef

The effect of an electric field on the rotating flows of a thin film using a perturbation technique

A M Morad[1,3], M Abu-Shady[1] and G I Elsawy[2]

[1] Department of Mathematics and Computer Science, Faculty of Science, Menoufia University, 32511 Egypt
[2] Faculty of Engineering, Modern Academy for Engineering and Technology, Cairo, Egypt

E-mail: dr_adel_morad@yahoo.com

Received 5 June 2019, revised 7 August 2019
Accepted for publication 12 September 2019
Published 31 December 2019

Abstract

The motion of a thin suspended film of an incompressible fluid under the effect of an external electric field is studied. The effects of the interfacial Maxwell stress, surface tension and intermolecular forces are studied, in which the forces are included in the Navier–Stokes equations. The perturbation technique is used to solve the given model. The obtained results show that, the fluid moves in a rotating pattern and the fluid particles move along the streamlines with different velocities. The free boundaries show good agreement with experimental data. In addition, the stability criteria are examined in the present model.

Keywords: electrohydrodynamics (EHD), thin films, mathematical modeling, perturbation techniques, orr-sommerfeld equation

(Some figures may appear in colour only in the online journal)

1. Introduction

Many scientific and industrial problems involve the flow of thin liquid films (see, for instance [1–8]). Thin film technology is used extensively in many applications including microelectronics, optics, magnetism, hard and corrosion resistant coatings, biotechnology, micro-mechanics, lasers, and medicine. Additionally, a new mathematical formulation of the electrohydrodynamics (EHD) of flows in a thin suspended liquid film was introduced in [9]. At larger scales the ascent of buoyant molten rocks (magma) below solid rocks and the spreading of lava on volcanoes are further problems of geological research [10–12]. Rotating thin films is crucial for mass transfer and heat, separation or mixing operations in diverse miniaturized technologies such as power generators in microfuel cells, sensors, lab-on-a-chip devices and drug delivery modules as introduced in [7].

Shirsavar *et al* [13] conducted an experiment on an electric current passing through a suspended film between two plates and created an electric generator in the liquid film. They named this experiment 'liquid film motor' which was presented in [13–15]. Recently, a theory for the rotation of suspended liquid film between two plates which rotates under the effect of an external electric field was introduced in [16]. Many works which include the motion form and the no slip boundary conditions are interpreted by this theory, such as [9, 14, 15].

In [9], the authors calculated an averaged rotating flow in a thin film by the edge effects in which the surface tension and the deviations of the free surfaces of a film from the planes were not considered. Additionally, their work showed that the jump of an electric field across a water dielectric interface can produce (due to electrokinetic effects) the tangential velocity of a fluid that, in turn, can maintain a steady rotating flow in the film. The effects of electric field generated stress (Maxwell stress), the free surface potential, surface tension, and the intermolecular van der Waals force have been studied in many works [17–20].

The aim of this paper is to study the EHD of a thin suspended liquid film where the flows are driven by a constant external electric field applied at the edges of the film in free surface flow. In the present model, the surface tension

[3] Author to whom any correspondence should be addressed.

and the deviations of the three dimensional free surfaces of a film from the planes are included which are not considered in recent works such as [7, 9].

This paper is divided into five sections as follows: In the first section, the characteristics of the physical system are presented. In the second section, the theoretical formulation of rotating flows in a square film is studied based on their velocity fields. In the third section, a dimensionless version of the given equations is obtained. The formulation of the present model and the results are given in the fourth and fifth sections.

2. Theoretical formulation

The rotating electrohydrodynamic flows in a suspended liquid film subject to an applied electric field at the edges of the film can be determined using the Navier–Stokes conservation of mass and momentum equations. The physical system under study consists of a rectangular thin liquid film with a free surface. The equation for the nonlinear evolution of the deforming surface is derived by considering both the hydrodynamic stresses and the Maxwell's stresses with appropriate boundary conditions.

The location of the free surface is represented by

$$z = h(x, y, t). \tag{2.1}$$

The external electric field leads to a Maxwell stress σ^M in the model. The total stress, $\boldsymbol{\sigma}^T$ is the combination of the Maxwell's stresses and the hydrodynamic stresses

$$\boldsymbol{\sigma}^T = \boldsymbol{\sigma}^M + \boldsymbol{\sigma}^H. \tag{2.2}$$

In the absence of magnetic field, $\boldsymbol{\sigma}^M$ can be written as

$$\boldsymbol{\sigma}^M = \varepsilon(\boldsymbol{EE} - 0.5(\boldsymbol{E}.\boldsymbol{E})\boldsymbol{I}). \tag{2.3}$$

Therefore, the components of the total stress tensor are

$$\sigma_{ij}^H = \mu\left(\frac{\partial v_i}{\partial x_j} + \frac{\partial v_j}{\partial x_i}\right) - \delta_{ij}p, \quad \sigma_{ij}^M = \varepsilon E_i E_j - \frac{1}{2}\varepsilon\delta_{ij}E_k E_k,$$

where, ε, p, δ_{ij}, and I are the fluid permittivity, pressure, Kronecker delta and unit matrix, respectively [21].

The total stress, $\boldsymbol{\sigma}^T$ can therefore be expressed as

$$\boldsymbol{\sigma}^T = \mu(\nabla\boldsymbol{v} + \nabla\boldsymbol{v}^T) - \left(p + \frac{\varepsilon|\boldsymbol{E}|^2}{2}\right)\boldsymbol{I} + \varepsilon\boldsymbol{EE}. \tag{2.4}$$

The corresponding electric field can be calculated as

$$\boldsymbol{E} = -\nabla\phi, \tag{2.5}$$

where ϕ is the electric potential. The first part in (2.4) is the viscid hydrodynamic contribution, and the second and third parts arise from interfacial electric field stresses given by the Maxwell stress tensor.

Along the shear line ($z = 0$), no-slip and no-penetration boundary conditions ($\boldsymbol{v} = 0$) are assumed. At the liquid free surface, $z = h(x, y, t)$, the normal and tangential stress balances are enforced and can be written as, respectively,

$$\boldsymbol{n}.\boldsymbol{\sigma}^T.\boldsymbol{n} = \gamma\kappa. \tag{2.6}$$

$$\boldsymbol{\tau}.\boldsymbol{\sigma}^T.\boldsymbol{n} = 0. \tag{2.7}$$

with the tangent vectors

$$\boldsymbol{\tau}^x = \frac{(1, 0, h_x)}{\sqrt{1 + h_x^2}}, \quad \boldsymbol{\tau}^y = \frac{(0, 1, h_y)}{\sqrt{1 + h_y^2}}, \tag{2.8}$$

and the normal vector pointing outward

$$\boldsymbol{n} = \frac{(-h_x, -h_y, 1)}{\sqrt{1 + h_x^2 + h_y^2}}, \tag{2.9}$$

where $\gamma\kappa$ is the capillary force with γ is the surface tension and $\kappa = Div\ \boldsymbol{n}$ is the local interfacial curvature of the film interface.

The location of the liquid-air free surface, $z = h(x, y, t)$ is defined by the following condition

$$-\frac{1}{|\nabla F|}\left(\frac{\partial F}{\partial t}\right) = \boldsymbol{v}.\boldsymbol{n}, \quad |\nabla F| = \left[\left(\frac{\partial F}{\partial x_i}\right)^2\right]^{1/2}, \tag{2.10}$$

where, $F(x, y, z, t) = z - h(x, y, t)$ is a single-valued function of x and y that vanishes on the surface and $\boldsymbol{v}$is the fluid velocity in Cartesian coordinates

$$\boldsymbol{v} = \boldsymbol{v}(\boldsymbol{x}, t), \quad \boldsymbol{v} = (u, v, w), \quad \boldsymbol{x} \equiv x_i = (x, y, z). \tag{2.11}$$

The dimensional equations governing the EHD of the incompressible flow of a Newtonian fluid are the mass and momentum conservation equations with the Maxwell and hydrodynamic stress contributions

$$\rho\left(\frac{\partial\boldsymbol{v}}{\partial t} + (\boldsymbol{v}.\nabla)\boldsymbol{v}\right) = -\nabla p + \nu\rho\Delta\boldsymbol{v} + Div\ \boldsymbol{\sigma}^M$$
$$= -\nabla p + \nu\rho\Delta\boldsymbol{v} + \varepsilon\Delta\phi\nabla\phi. \tag{2.12}$$

The continuity equation is

$$Div\ \boldsymbol{v} = 0, \tag{2.13}$$

and the velocities satisfy the no-slip and no-penetration boundary condition

$$\boldsymbol{v} = 0.$$

The charge density is determined by summing the concentration distributions c_k

$$\rho_e = Fa\sum_k e_k c_k. \tag{2.14}$$

Here, Fa denotes Faraday's constant, and e_k is the valence number of the kth species. This charge distribution along with the external applied electric potentials generate an electric field within the liquid that can be determined from the Poisson–Boltzmann relation

$$Div\ (\varepsilon\boldsymbol{E}) = q. \tag{2.15}$$

Here, $\boldsymbol{v}$ is the flow velocity ($\mathrm{m\,s^{-1}}$), p is the pressure ($\mathrm{N\,m^{-2}}$), ρ is the liquid density ($\mathrm{kg\,m^{-3}}$), q is the charge density ($\mathrm{C\,m^{-3}}$), ϕ is the electric potential (V), $\boldsymbol{E}$ is the electric field strength ($\mathrm{V\,m^{-1}}$), c_k is the molar concentration for the kth component of a mixture ($\mathrm{mol\,m^{-3}}$), $\boldsymbol{i}_k$ is the density fluxes of the concentrations ($\mathrm{molm^{-2}\,s^{-1}}$), ν is the kinematic viscosity (m^2/s), e_k are the electric charges of the components (in the units of the electron charge), ε is the permittivity of the liquid $\varepsilon = \varepsilon_r\varepsilon_0$, where ε_r is the relative permittivity and ε_0 is the absolute permittivity, $\mathrm{C\,V^{-1}\,m^{-1}}$, and Fa is the Faraday constant ($\mathrm{C\,mol^{-1}}$). In addition, we define D_k and γ_k as the molecular diffusivity ($\mathrm{m^2\,s^{-1}}$) and electric mobilities ($\mathrm{m^2\,V^{-1}\,s^{-1}}$) for the components of a mixture, respectively. Using differential geometry, the surface curvature can be written as

$$\kappa = \frac{(h_{xx} + h_{yy}) + (h_{xx}h_y^2 + h_{yy}h_x^2) - 2h_xh_yh_{xy}}{(1 + h_x^2 + h_y^2)^{3/2}}.$$

The second boundary condition at the free surface (called 'kinematic') is formulated by considering that a fluid particle on the free surface remains on the surface. Therefore, executing the dot product $\boldsymbol{v}.\boldsymbol{n}$, the condition (2.10) can be rewritten as

$$w = h_t + uh_x + vh_y \quad \text{on} \quad z = h(x, y, t). \tag{2.16}$$

The normal and tangential components of the viscous stress vector at the interface, in which n_i, and $\tau_i^{(k)}$ are the i–direction components of unit vectors, are the outward component normal to the free surface and the two tangential components to the free surface in the (x, z) and (y, z) planes, respectively,

$$\sigma_n \equiv n_i\sigma_{ji}^T n_j = \gamma\kappa, \quad \sigma_\tau^{(k)} \equiv \tau_i^{(k)}\sigma_{ji}^T n_j = 0, \quad k = x, y. \tag{2.17}$$

Equation (2.16) represents a nonlinear boundary condition; the free surface h is an unknown function of time and space and must be determined as part of the solution. Using the relations (2.1)–(2.9), the dynamic boundary conditions (2.6) and (2.7) are written as

$$\sigma_\tau^{(x)} = \frac{(\sigma_{13} + \sigma_{33}h_x) - h_x(\sigma_{11} + \sigma_{31}h_x) - h_y(\sigma_{12} + \sigma_{32}h_x)}{\sqrt{1 + h_x^2}\sqrt{1 + h_x^2 + h_y^2}} \tag{2.18}$$

$$\sigma_\tau^{(y)} = \frac{(\sigma_{23} + \sigma_{33}h_y) - h_x(\sigma_{21} + \sigma_{31}h_y) - h_y(\sigma_{22} + \sigma_{32}h_y)}{\sqrt{1 + h_y^2}\sqrt{1 + h_x^2 + h_y^2}} \tag{2.19}$$

$$\begin{aligned}&\mu[(1 - h_x^2)(u_z + w_x) + 2h_x(w_z - u_x)\\ &\quad - h_y(u_y + v_x) - h_xh_y(v_z + w_y)]\\ &\quad + \varepsilon(\phi_x\phi_z(1 - h_x^2) - h_xh_y\phi_y\phi_z - h_y\phi_x\phi_y) = 0\end{aligned} \tag{2.20}$$

$$\begin{aligned}&\mu[(1 - h_y^2)(v_z + w_y) + 2h_y(w_z - v_y)\\ &\quad - h_x(u_y + v_x) - h_xh_y(u_z + w_x)]\\ &\quad + \varepsilon(\phi_y\phi_z(1 - h_y^2) - h_xh_y\phi_x\phi_z - h_x\phi_x\phi_y) = 0\end{aligned} \tag{2.21}$$

for the tangential directions and

$$\begin{aligned}&-p + \frac{2\nu\rho}{1 + h_x^2 + h_y^2}(w_z - h_x(u_z + w_x) - h_y(v_z + w_y)\\ &\quad + h_x^2u_x + h_xh_y(v_x + u_y) + h_y^2v_y)\\ &\quad + \frac{\varepsilon}{1 + h_x^2 + h_y^2}(h_x^2\phi_x^2 + h_y^2\phi_y^2 + h_z^2\phi_z^2\\ &\quad - 2h_xh_y\phi_x\phi_y - 2h_y\phi_y\phi_z - 2h_x\phi_x\phi_z)\\ &= \gamma\frac{h_{xx}(1 + h_y^2) - 2h_xh_yh_{xy} + h_{yy}(1 + h_x^2)}{(1 + h_x^2 + h_y^2)^{3/2}}\end{aligned} \tag{2.22}$$

for the normal direction.

For small slopes, the tangent and normal vectors and the curvature can be written in the following form

$$\begin{aligned}&\boldsymbol{\tau}^x \simeq (1, 0, h_x), \quad \boldsymbol{\tau}^y \simeq (0, 1, h_y),\\ &\boldsymbol{n} \simeq (-h_x, -h_y, 1), \quad \text{and} \quad \kappa \simeq h_{xx} + h_{yy}\end{aligned} \tag{2.23}$$

so that the balance of the normal component and the two tangential stress components at the free interface $z = h(x, y, t)$ may be described conveniently by

$$\nu\rho(u_z + w_x) + \varepsilon(\phi_x\phi_z - h_y\phi_x\phi_y) = 0 \tag{2.24}$$

$$\nu\rho(v_z + w_y) + \varepsilon(\phi_y\phi_z - h_x\phi_x\phi_y) = 0 \tag{2.25}$$

$$-p + 2\nu\rho w_z - 2\varepsilon(h_y\phi_y\phi_z + h_x\phi_x\phi_z) = \gamma(h_{xx} + h_{yy}). \tag{2.26}$$

3. Dimensionless equations

For the dimensionless variables, we utilize the following transformations to render the problem dimensionless

$$[x, y] = a_*, \quad [z, h] = h_*, \quad \text{and} \quad [t] = \mathcal{T}_*. \tag{3.1}$$

The velocities, on the other hand, scale as

$$[u, v] = \frac{a_*}{\mathcal{T}_*}, \quad \text{and} \quad [w] = \frac{h_*}{\mathcal{T}_*}. \tag{3.2}$$

where, a_* is the characteristic length in the plane of the film, h_* is the dimensional half thicknesses of the film and $\mathcal{T}_*$ is the characteristic time.

The molar concentration, electric field, electric potential, charge density and pressure are dimensionalized as, respectively,

$$\begin{aligned}&[c_k] = \mathcal{C}_*, \quad [\boldsymbol{E}] = \mathcal{E}_*, \quad [\phi] = \mathcal{E}_*a_*,\\ &[q] = F_*\mathcal{C}_*, \quad \text{and} \quad [p] = F_*\mathcal{C}_*\mathcal{E}_*a_*\delta^2,\end{aligned} \tag{3.3}$$

with the quantities

$$\begin{aligned}&\Upsilon = \frac{F_*\mathcal{E}_*a_*}{R_*T_*}, \quad \mathcal{T}_*^2 = \frac{\rho_*a_*}{F_*\mathcal{C}_*\mathcal{E}_*\delta^2},\\ &\delta^2 = \frac{h_*^2}{a_*^2} \quad \text{and} \quad \gamma_* = \gamma F_*\mathcal{C}_*\mathcal{E}_*a_*^2\delta^2.\end{aligned} \tag{3.4}$$

Here, $\mathcal{C}_*$ is the molar concentration, $F_*\mathcal{C}_*$ is the characteristic charge density, $\mathcal{E}_* a_*$ is the characteristic difference in the electric potentials in the x direction, R_* is the universal gas constant, and T_* is the absolute temperature of a solution.

The dimensional values of the kinematic viscosity ν_*, diffusion coefficients D_k^*, and dielectric permittivity ε_* are linked to their dimensionless counterparts by

$$\nu = \frac{\nu_* \mathcal{T}_*}{a_*^2}, \quad D_k = \frac{D_k^* \mathcal{T}_*}{a_*^2}, \quad \text{and} \quad \varepsilon = \frac{\varepsilon_* \mathcal{E}_*}{a_* F_* \mathcal{C}_*}. \tag{3.5}$$

The governing equations describing the EHD flows of a multicomponent fluid are converted into the following dimensionless forms by choosing the references scales listed above

$$\delta^2 \frac{D\boldsymbol{u}}{Dt} = -\delta^2 \nabla_0 p + \delta^2 \nu \Delta_0 \boldsymbol{u} + \nu \partial_{zz} \boldsymbol{u} - q \nabla_0 \phi, \tag{3.6}$$

$$\delta^4 \frac{Dw}{Dt} = -\delta^2 \partial_z p + \delta^4 \nu \Delta_0 w + \delta^2 \nu \partial_{zz} w - q \partial_z \phi, \tag{3.7}$$

$$Div\ {}_0\boldsymbol{u} + \partial_z w = 0, \tag{3.8}$$

$$\varepsilon(\delta^2 \Delta_0 \phi + \partial_{zz} \phi) = -\delta^2 q, \quad q = \sum_k e_k c_k. \tag{3.9}$$

The nondimensional form of the conservation equations of a mixture is

$$\delta^2 \frac{Dc_k}{Dt} + \delta^2\, Div\ {}_0\boldsymbol{i}_k + \partial_z \boldsymbol{I}_k = 0, \tag{3.10}$$

$$\boldsymbol{i}_k = -D_k(\nabla_0 c_k + e_k \Upsilon c_k \nabla_0 \phi), \tag{3.11}$$

$$\boldsymbol{I}_k = -D_k(\partial_z c_k + e_k \Upsilon c_k \partial_z \phi). \tag{3.12}$$

The material derivative, the gradient and the horizontal Laplacian operator in the xy plane can be expressed as, respectively,

$$\frac{D}{Dt} = \partial_t + \boldsymbol{u}.\nabla_0 + w\partial_z, \quad \nabla_0 = (\partial_x, \partial_y), \quad \text{and}$$
$$\Delta_0 = (\partial_{xx}, \partial_{yy}). \tag{3.13}$$

Here, $\boldsymbol{v} = (\boldsymbol{u}, w)$ is the velocity field and $\boldsymbol{u} = (u, v)$ are their x and y projections, $\boldsymbol{i}_\mathrm{k}$ and $\boldsymbol{I}_\mathrm{k}$ are the planar and transversal density fluxes of the concentrations, and the parameter Υ characterizes the ratio of the transport of concentrations by an electric field and by diffusion.

The corresponding dimensionless version of the boundary conditions is:

On the film boundaries:

$$u = v = w = 0. \tag{3.14}$$

The no-leak conditions for concentrations are:

$$\boldsymbol{I}_k|_{z=-1} = 0, \quad \boldsymbol{I}_k|_{z=+h} = 0. \tag{3.15}$$

The vanishing normal electric current is:

$$\partial_z \phi|_{z=-1} = 0, \quad \partial_z \phi|_{z=+h} = 0. \tag{3.16}$$

The kinematic condition (2.16) at the free surface $z = h$ (x, y, t) is the following:

$$w = \partial_t h + u\partial_x h + v\partial_y h. \tag{3.17}$$

Using the condition (3.16), the continuity of the shear and normal stresses (2.24)–(2.26) at the free surface $z = h(x, y, t)$ can be written as, respectively,

$$\delta^2 \nu(u_z + \delta^2 w_x) + \epsilon(\phi_x \phi_z - \delta^2 h_y \phi_x \phi_y) = 0, \tag{3.18}$$

$$\delta^2 \nu(v_z + \delta^2 w_y) + \epsilon(\phi_y \phi_z - \delta^2 h_x \phi_x \phi_y) = 0, \tag{3.19}$$

$$-\delta^2 p + 2\delta^2 \nu w_z - 2\epsilon(h_y \phi_z \phi_y + h_x \phi_z \phi_x) = \gamma \delta^3 (h_{yy} + h_{xx}). \tag{3.20}$$

The dimensionless form of the Navier–Stokes equation (2.12) with the Maxwell and hydrodynamic stress contributions can be written as

$$\delta^2 \frac{D\boldsymbol{u}}{Dt} = -\delta^2 \nabla_0 p + \delta^2 \nu \Delta_0 \boldsymbol{u} + \nu \partial_{zz} \boldsymbol{u} + \varepsilon\left(\Delta_0 \phi + \frac{1}{\delta^2} \partial_{zz} \phi\right) \nabla_0 \phi, \tag{3.21}$$

$$\delta^4 \frac{Dw}{Dt} = -\delta^2 \partial_z p + \delta^4 \nu \Delta_0 w + \delta^2 \nu \partial_{zz} w + \varepsilon\left(\Delta_0 \phi + \frac{1}{\delta^2} \partial_{zz} \phi\right) \partial_z \phi. \tag{3.22}$$

4. Formulation of the model

4.1. The total electric potential and velocity

The electric potential field in the system is developed as a superposition of three potential fields. The first field is due to the formation of the internal potential and is represented by the potential $\phi_1(z)$. The second and the third fields are due to the external electric field E_0, which are represented as a gradient of the potential $\phi_2(x)$, $\phi_3(y)$. Then the total electric potential can be written as

$$\phi(x, y, z) = \phi_1(z) + \phi_2(x) + \phi_3(y). \tag{4.1}$$

Upon using the classical Poisson–Boltzmann relation, the potential distribution is obtained as

$$\phi_{zz} = -\frac{\delta^2}{\epsilon} q, \frac{q}{\epsilon} = \rho, \tag{4.2}$$

where, ρ is the charge density and ϵ is the dielectric permittivity, such that the charge density follows the Boltzmann distribution.

Thus, the total electric potential can be obtained as

$$\phi(x, y, z) = -\frac{x}{e_1} - \frac{y}{e_2} + \left(\frac{1}{\mathrm{Sinh}\left(\frac{h\delta}{D_n}\right)}\right)\left(Z_P \,\mathrm{Sinh}\left(\frac{z\delta}{D_n}\right) + \mathrm{Sinh}\left(\frac{\delta}{D_n}(h - z)\right)\right), \tag{4.3}$$

where the Debye number is written as an equation of the Debye length and the film thickness as

$$D_n = \frac{\lambda_d}{H}.$$

The Debye length depends on the ionic concentration as

$$\lambda_d \propto \frac{1}{\sqrt{C_k}},$$

where C_k is the ionic concentration, and e_1 and e_2 are the external electric fields in the x direction and y direction, respectively.

Now, we can define the zeta potential ratio, Z_P, one of the most important functions of our study:

$$Z_P = \frac{\eta_{\text{interface}}}{\eta_{\text{film}}},$$

where $\eta_{\text{interface}}$ is the potential of the interface and η_{film} is the potential of the film. Z_P at the free surface is a function of a variety of parameters involving the fluid and interface properties as introduced in [21]. The solution of the model equation at the boundaries can be obtained by using the uniform property of the thin film thickness. Therefore, the basic equations can be formulated for the initial velocity $U(z)$ as follows

$$\nu\partial_{zz}U = q\phi_x, \tag{4.4}$$

with boundary condition

$$\nu\partial_z U + \epsilon\phi_x\phi_z = 0, \tag{4.5}$$

and then the fluid velocity at the free surface is

$$U = \left(\frac{\epsilon}{\delta^2\nu e_1}\right)\mathrm{Csch}\left(\frac{h\delta}{D_n}\right)\left(-\mathrm{Sinh}\left(\frac{h\delta}{D_n}\right) + \mathrm{Sinh}\left(\frac{(h - z)\delta}{D_n}\right) + \mathrm{Sinh}\left(\frac{z\delta}{D_n}\right)Z_P\right).$$

Figure 1 shows that the initial velocity exhibits the same behaviour under the surface for different values of the surface zeta potential, Z_P and then changes on the surface. This behaviour produced what is called interfacial stress. During the study of the system stability, the interfacial stress was detected by the interfacial polarity. Furthermore, the system is stable at the positive values $Z_P = 0.5$ and $Z_P = 1$, as shown in figure 1 (curves 1 and 2). However, the negative values $Z_P = -0.5$ and $Z_P = -1$ make the system unstable, as shown in figure 1 (curves 1 and 2). The interfacial polarity with respect to the zeta potential controls the system stability, as it reduces the interfacial stress.

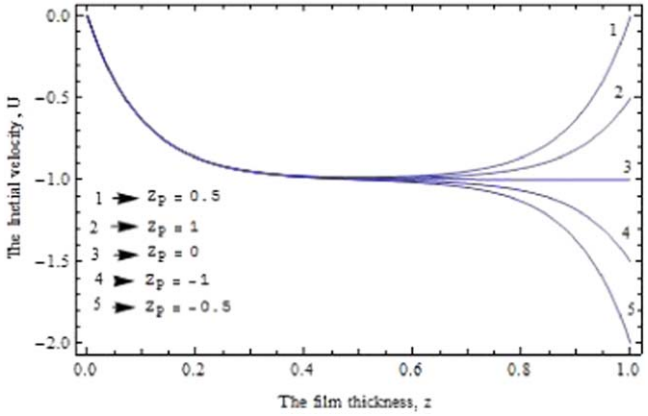

Figure 1. The initial velocity is plotted as a function of the wave-number for different values of the surface zeta potential ratio, Z_P at $D_n = 0.1$.

4.2. Normal mode analysis

The perturbation of the variables is as follows:

$$u(x, y, z) = U(z) + \bar{u}(x, z, y),$$
$$v(x, y, z) = \bar{v}(x, z, y),$$
$$w(x, y, z) = \bar{w}(x, z, y),$$
$$h(x, y, t) = h + \bar{h}(x, y),$$

where the bare variables correspond to the perturbation. Using normal mode analysis with the perturbation parameters, the stream function is given as

$$\tilde{\psi}(x, y, z, t) = \psi(z)\mathrm{e}^{\mathrm{i}k(x+y-ct)},$$
$$\bar{h}(x, y) = H_0\mathrm{e}^{\mathrm{i}k(x+y-ct)},$$

where k is the wave-number and c is the wave velocity.

4.3. Derivation of the model

The model equation is obtained by using a derivation of the Navier–Stokes equations; then, the final equation becomes

$$\delta^2(uu_{xz} + wu_{zz} - \delta^2 w_{tx} + u_{tz} - \delta^2 uw_{xx}) + q_x\phi_z - q_z\phi_x + \nu(\delta^2 u_{xxz} + \delta^2 u_{yyz} + u_{zzz} - \delta^4 w_{xxx} - \delta^4 w_{yyx} - \delta^2 w_{zzx}) = 0. \tag{4.6}$$

Eliminating the pressure from the Navier–Stokes equations, we obtain

$$\delta^2(u_t + uu_x + wu_z) - 2\epsilon(h_{xx}\phi_x\phi_z + h_{yx}\phi_y\phi_z) + q\phi_x - \nu(\delta^2 u_{xx} + \delta^2 u_{yy} + u_{zz} - 2\delta^2 w_{xz}) = \gamma\delta^3(h_{xxx} + h_{yyx}). \tag{4.7}$$

4.4. The Orr-Sommerfeld equations

The Orr-Sommerfeld equations are obtained by using the perturbation technique as shown in [18], and then the model equation describing the thin film moving with the initial

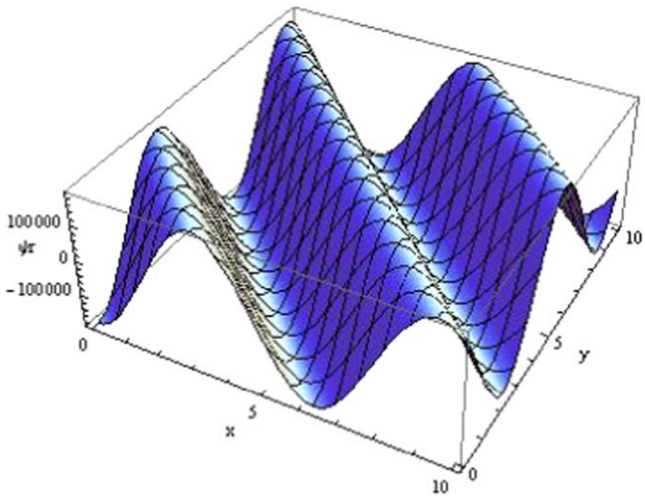

Figure 2. The stream function is plotted as a function of the wavenumber, k and the surface tension, γ.

velocity under the effect of an electric field is given by

$$\bar{u} = \frac{\partial \tilde{\psi}}{\partial z} = \mathrm{D}\psi \mathrm{e}^{\mathrm{i}k(x+y-ct)}$$

$$\bar{w} = \frac{\partial \tilde{\psi}}{\partial x} = \mathrm{i}k\psi(z)\mathrm{e}^{\mathrm{i}k(x+y-ct)}.$$

After substitution with $\bar{u}$ and $\bar{w}$, we obtain the mathematical model, which is given by

$$\left(\nu\left(\left(D^2 - \frac{3}{2}k^2\delta^2\right)^2 - \frac{\delta^4 k^4}{4}\right) - \mathrm{i}k\delta^2((U-c)(D^2 - k^2\delta^2)) - D^2U)\psi(z) + q_x\phi_z - q_z\phi_x = 0, \tag{4.8}$$

the boundary conditions for the normal direction

$$\nu D(D^2 - 4k^2\delta^2) - \mathrm{i}k\delta^2((U-c)D\psi(h) - \psi(h)DU) = q\phi_x + 2k^2H_0(i\gamma\delta^3 k + \epsilon(\phi_x + \phi_y)\phi_z), \tag{4.9}$$

and the tangential direction

$$\nu\delta^2(D^2 + k^2\delta^2)\psi(h) + \epsilon(\phi_x\phi_z - \mathrm{i}k\delta^2 H_0\phi_x\phi_y) = 0, \tag{4.10}$$

and the kinematic condition

$$\psi(h) + H_0(U-c) = 0, \tag{4.11}$$

where D is the derivative of $\psi(z)$.

The solution of the eigenvalue problem is obtained by considering an expansion of the eigenvalue and the eigenfunction around their solutions for

$$c = c_0 + \mathrm{i}kc_1$$

$$\psi = \psi_0 + \mathrm{i}k\psi_1.$$

The solution of the Orr-Sommerfeld equation is obtained using the perturbation expansion method.

The set of equations with zero order are given by

$$\nu(D^4\psi) = q_z\phi_x - q_x\phi_z \tag{4.12}$$

with the boundary conditions

$$\nu D^3\psi(h) = q\phi_x, \tag{4.13}$$

$$\nu\delta^2 D^2\psi(h) = -\epsilon\phi_x\phi_z, \tag{4.14}$$

$$\nu D\psi(0) = 0, \tag{4.15}$$

$$\nu\psi(0) = 0. \tag{4.16}$$

By solving the above set of equations, we obtain

$$\psi_0 = -\frac{z\epsilon}{\nu\delta^2 e_1} + \frac{\epsilon\,\mathrm{Csch}\left(\frac{h\delta}{D_n}\right)\left(\mathrm{Cosh}\left(\frac{h\delta}{D_n}\right) - \mathrm{Cosh}\left(\frac{(h-z)\delta}{D_n}\right) - Z_P + \mathrm{Cosh}\left(\frac{z\delta}{D_n}\right)Z_P\right)D_n}{\delta^3\nu e_1} \tag{4.17}$$

$$c_0 = -\frac{h\epsilon}{\nu\delta^2 e_1 H_0} + \frac{\epsilon\,\mathrm{Csch}\left(\frac{h\delta}{D_n}\right)\left(-1 + \mathrm{Cosh}\left(\frac{h\delta}{D_n}\right) - Z_P + \mathrm{Cosh}\left(\frac{h\delta}{D_n}\right)Z_P\right)D_n}{\delta^3\nu e_1 H_0} + \frac{\epsilon}{\nu e_1\delta^2}(Z_P - 1). \tag{4.18}$$

The set of equations with first order is given by

$$\nu(D^4\psi) = \delta^2((U-c_0)D^2\psi_0(z) - \psi_0(z)D^2U)$$

with the boundary conditions

$$\nu D^3\psi(h) = -\delta^2(\psi_0(h)DU - (U-c_0)D\psi_0(h) - 2\gamma H_0\delta k^2),$$

$$\nu\delta^2 D^2\psi(H) = \epsilon\delta^2\phi_x\phi_y H_0,$$

$$\nu D\psi(0) = 0,\ \nu\psi(0) = 0.$$

Then, we obtain $\nu\,\psi_1$ as an expansion such that

$$\nu\psi_1 = A_0 + A_1D_n + A_2{D_n}^2 + A_3D_n^3 + A_4D_n^4. \tag{4.19}$$

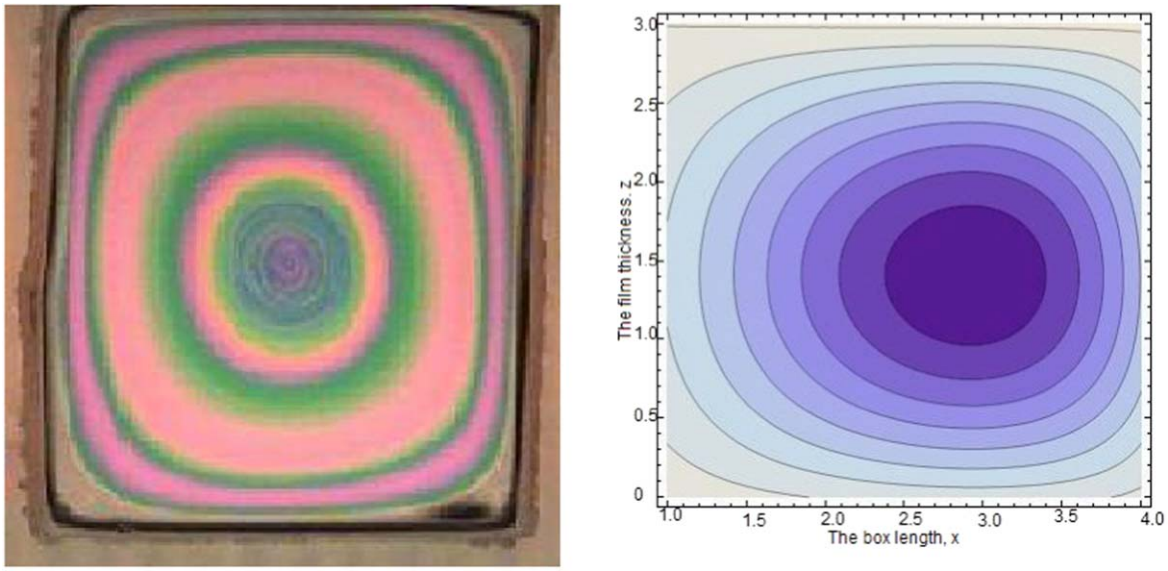

Figure 3. The left graph correspond to the rotation of the thin film in a laboratory experiment (liquid film motor) [13]. The right graph describes the rotation of the thin film in our model.

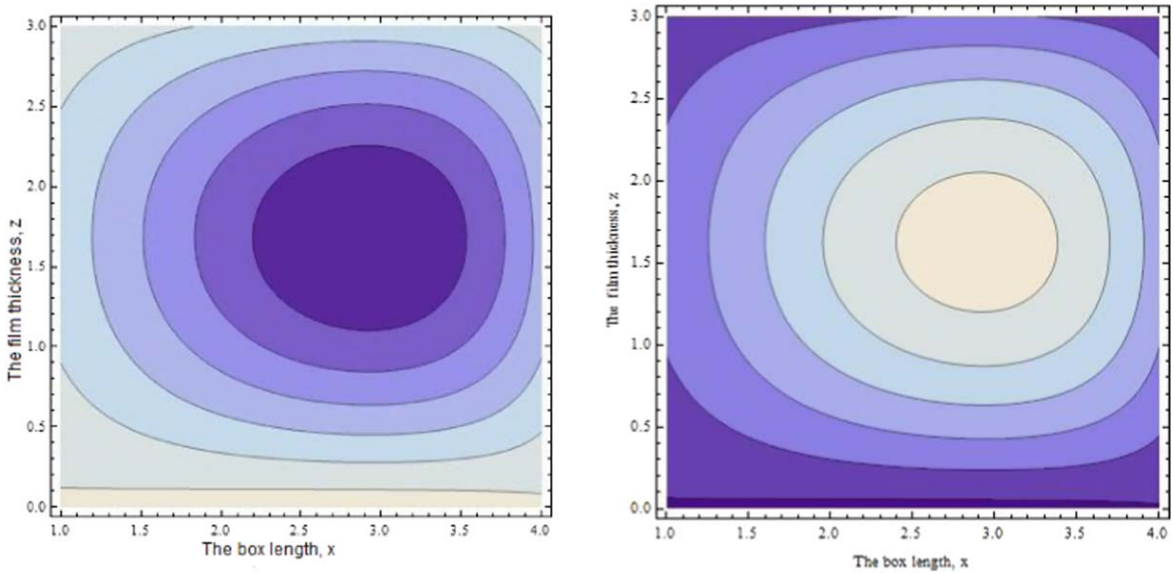

Figure 4. The stream lines of the rotating film at $t = 5$ s (the left graph) and at $t = 10$ s (the right graph), $D_n = 0.5$, $Z_p = 1$, $e_1 = 100$ and $e_2 = 100$.

We can obtain c_1 from the kinematic boundary condition as

$$c_1 = \frac{\psi_1}{H_0},$$

Therefore, c_1 can be expanded as follows

$$c_1 = B_0 + B_1 D_n + B_2 {D_n}^2 + B_3 {D_n}^3 + B_4 {D_n}^4. \qquad (4.20)$$

The solutions of c_1 and ψ_1 are calculated in appendix A.

5. Results and discussion

5.1. The stream function

After the solution of the zero- and first-order Orr-Sommerfeld equations, the stream function becomes

$$\tilde{\psi}(x, y, z, t) = (\psi_0 + \mathrm{i}k\psi_1)\mathrm{e}^{\mathrm{i}k(x+y-c_0 t)+k^2 c_1 t}. \qquad (5.1)$$

Figure 2 shows the three dimensional behaviour of the stream function with the surface tension and the wave-number.

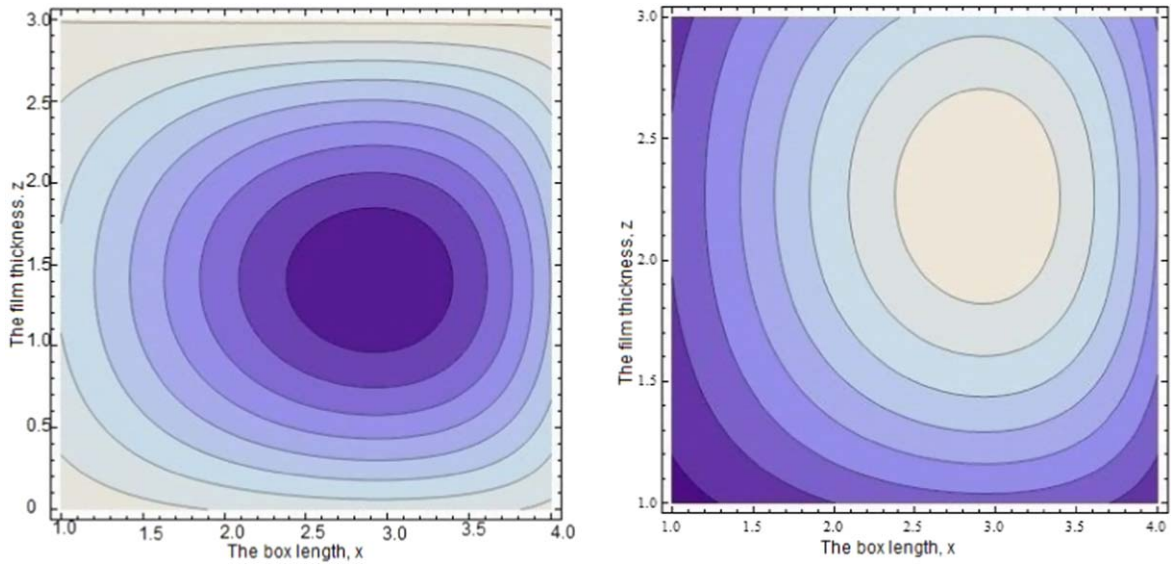

Figure 5. The stream lines of the rotating film at $t = 15$ s (the left graph) and at $t = 20$ s (the right graph), $D_n = 0.5$, $Z_p = 1$, $e_1 = 100$ and $e_2 = 100$.

This behaviour can be observed through the effect of the local curvature. Thus, the external electric field appears, according to which the thin suspended film rotates.

Good reviews related to fully formed rotation in thin liquid film [13]. The rotating film can be seen in figure 3 (the left graph). In this fluid regime, the rotation of suspended liquid film between two plates which rotates under the effect of an external electric field, all patterns which are also observed in the proposed model as in figures 3 (the right graph). This gives good agreement between the experiment and the rotation of the thin suspended film in our model.

Figure 4 shows the rotation of the thin film during the first interval [5, 10]. The rotation of the thin film appears in the figure is depended on the angular velocity at different moments of time.

Figure 5 shows the rotation of the thin film during the second interval [15, 20]. The figures of the stream function show the rotating of the thin suspended film as the stream function equation describes the movement of the thin film by containing the wave-number and the wave velocity. The thin suspended film rotates when the external electric field urges free charge on the surface of the thin film that pushes the current stimulates on the free surface charge generating the thin film motion as introduced in [15]. When the external electric field is connected at the edges of the thin film, the waves of the thin film acquire variable angular velocity. At the begging of the motion, the angular velocity of the fluid will be maximum at the edges. At the first interval, the angular velocity of the fluid moves up to reach the maximum at the centre. When the angular velocity reaches the maximum at the centre, it moves again in the direction of the edges until the maximum speed returns again to the edges as described in figure 4. In the second interval, the thin suspended film has completed an interval and the fluid in a state of stability and is identical to what happens in the laboratory experiment as introduced in [13] (see figure 5). In [9, 16], authors are demonstrated the electrohydrodynamic of a thin suspended liquid film where the flows are given by constant electric field at the edges of the film using averaging method. Comparing the results of our model and the results in [9, 16], a great match in the graphics and their physical interpretation is in favour of the proposed model as shown in figure 3. The proposed model is superior in terms of studying the thin film motion in three dimension at free surface flow. In addition, it outperforms the previous models in terms of the impact of many variables on the system stability.

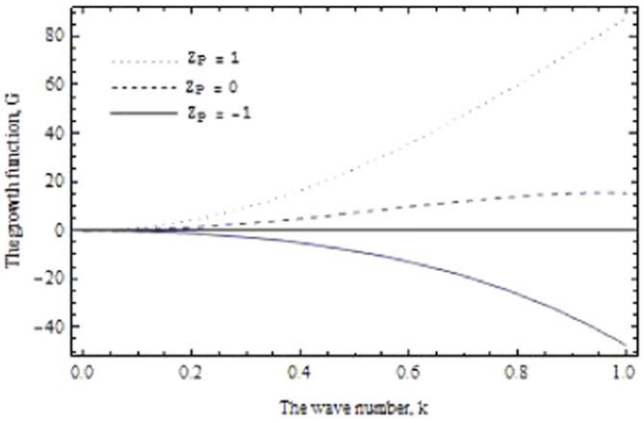

Figure 6. The growth rate function is plotted as a function of the wave-number for different values of Z_P and $\gamma = 10$.

5.2. The real part of the growth rate function

The real part of the growth rate function is obtained from the solution of the Orr-Sommerfeld equations

$$G = k^2 g(Z_P, D_n, \epsilon, \nu, \delta, e_1, e_2) + f(\gamma)k^4, \qquad (5.2)$$

where

$$f(\gamma) = -\frac{2}{3\nu}h^3\delta^3\gamma,$$

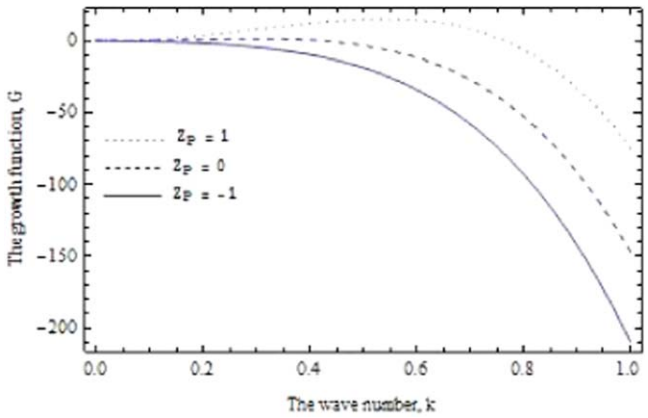

Figure 7. The growth rate function is plotted as a function of the wave-number for different values of Z_P and $\gamma = 30$.

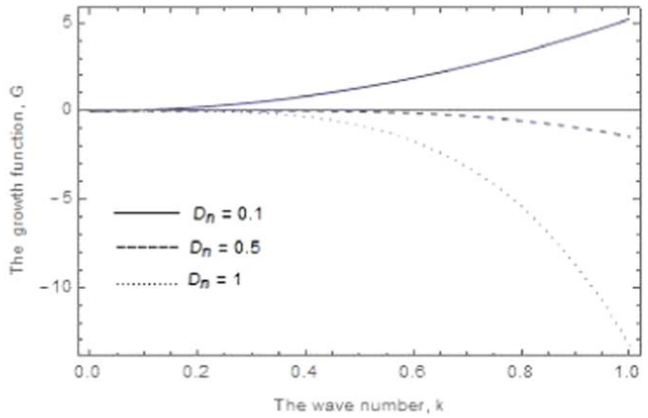

Figure 8. The growth rate function is plotted as a function of the wave-number for different values of D_n.

where k^2c_1 is equivalent to the real part of the growth function. The growth rate function has many variables through which the effect of a external electric field can be studied and a natural interpretation can be achieved. The stability can be studied for different values of the wave-number. Mayur *et al* [18] used Orr-Sommerfeld equation as a method of solution in two dimension. In the present model we have generalized the problem to three dimension, which led to a growth function that is rich in variables.

$$G = F_0 + F_1 D_n + F_2 {D_n}^2 + F_3 {D_n}^3 + F_4 {D_n}^4.$$

The solution of G is calculated in appendix B.

5.3. The growth rate function for different values of the interface zeta potential ratio

Figure 6 shows that the growth rate function exhibits the same behaviour under the surface for different values of Z_P and then changes on the surface. This behaviour produced what is called interfacial stress. The interfacial polarity reveals the interfacial stress in the system stability in the equation of the real part of the growth rate. In addition, the interfacial polarity with respect to the interface zeta potential controls the system stability, as it reduces the interfacial stress when Z_P is negative (with the opposite polarity to the surface) and makes the system unstable. However, at positive Z_P (with the same polarity as the surface) makes the system more stable. This gives good agreement with the figure of the initial velocity with Z_P as shown in figure 1. Figure 7 shows that the growth rate function becomes unstable at large values of the surface tension regardless of the values of Z_P.

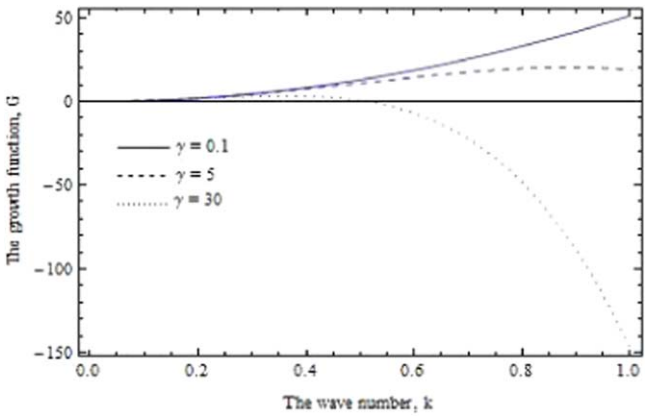

Figure 9. The growth rate function is plotted as a function of the wave-number for different values of the surface tension.

5.4. The growth rate function for different values of the Debye number

Figure 8 shows the effect of the Debye number, D_n on the stability of the system, which can be explained by the thin film thickness and the Debye length, λ_d. The fluid is more stable by increasing the value of D_n which is achieved by decreasing the thin film thickness and increasing λ_d. Notwithstanding, increasing the ionic concentration due to the external electric field makes the system unstable. The value of D_n can be considered as an indirect variable to study the effect of the external electric field. It should be noted that both the thin film thickness and Debye length have no effect when the film thickness is in the same range of λ_d. We have exploited the model introduced in [18] to treat the general case at the boundary conditions with Maxwell and hydrodynamic stresses: local curvature and surface tension. Based on the detailed analysis and simulations tests, we found that the behaviour of the thin film becomes more stable.

5.5. The growth rate function for different values of the surface tension

Figures 9 and 10 show the effect of the surface tension on the stability of the system. The surface tension has a significant effect at large values; however there is no noticeable at small values as shown in figure 9. The large values of surface tension increases the interfacial stability at small values of the wave-number. When the wave-number takes values from 0 to 0.4, the thin film is stable and there is no significant effect of the surface tension. However, for the values from 0.4 to 1 of the wave-number and small values of the surface tension, the motion of the thin film tends to stability. The final case, when the wave-number takes values from 0.4 to 1 and the surface

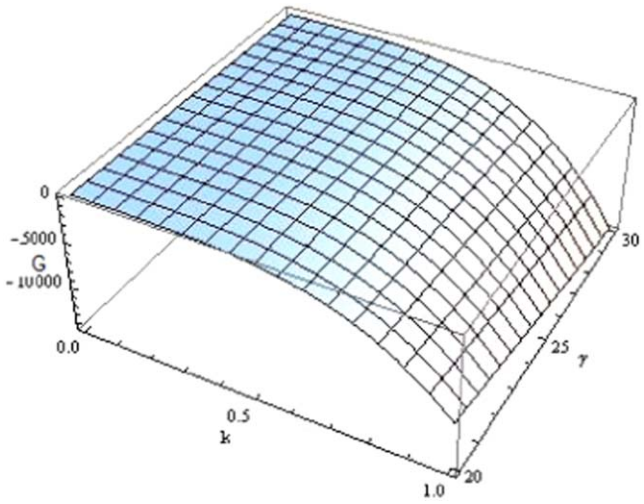

Figure 10. The growth rate function is plotted as a function of the wave-number and surface tension.

tension at large values, the surface tension makes the system unstable. This gives a good agreement with the results obtained in [22, 23]. By using the values of the variables in the mathematical model that is introduced in [18], we found that the growth function follows the same behaviour in the absence of surface tension in their model. Therefore, there is no significant effect on the behaviour of the growth function with surface tension at the case in [18]. Summarizing, the effect of the surface tension at large values makes the thin film unstable as shown in figure 10.

6. Conclusion

This paper has been presented the motion of a thin suspended film of an incompressible fluid under the effect of an electric field. Based on depth-averaged and multi-scale asymptotic expansion methods the Orr-Sommerfeld model for this electrohydrodynamic system has been deduced. The perturbation technique is used to solve the present model, in which the model is generalized to 3D space. In addition, we have investigated periodic solutions of the obtained model in different cases of instability to characterize the behaviour of the thin suspended film. Many variables affect the stability of the system, including the Debye number, D_n, the zeta potential, Z_P and the surface tension, S. The stability of the fluid can be increased by increasing the value of D_n that is achieved by decreasing the thin film thickness and increasing the Debye length, λ_d. The interfacial polarity with respect to the zeta potential controls the system stability, as it reduces the interfacial stress when Z_P is negative (with the opposite polarity as the surface), making the system more unstable. At positive case of Z_P (with the same polarity as the surface), the system is more stable, as observed in [24, 25]. The surface tension has significant effect only at large values. The results indicate that the system reveals unstable behaviour characterized by the perturbations in the linear region, as observed in [26–28]. Good agreement between the theory in the presence of free boundaries is found with the experiments in [9, 16]. Additionally, we confirmed our study by list of graphical models that illustrate the stability of the thin film system.

Appendix A

Coefficients of the terms in the expansion of $(\nu\ \psi_1)$ are

$$\begin{aligned}A_0 = &\frac{hz^2\epsilon^2\mathrm{Csch}\left(\frac{h\delta}{D_n}\right)^2}{2\delta^2\nu^2e_1^2} - \frac{z^3\epsilon^2\mathrm{Csch}\left(\frac{h\delta}{D_n}\right)^2}{6\delta^2\nu^2e_1^2} \\ &+ \frac{h^2z^2\epsilon^2}{2\delta^2\nu^2e_1^2H_0} - \frac{hz^3\epsilon^2}{6\delta^2\nu^2e_1^2H_0} \\ &- hk^2z^2\gamma\delta^3H_0 + \frac{1}{3}k^2z^3\gamma\delta^3H_0 + \frac{z^2\epsilon H_0}{2e_1e_2} \\ &- \frac{hz^2\epsilon^2Z_P}{\delta^2\nu^2e_1^2} + \frac{z^3\epsilon^2Z_P}{6\delta^2\nu^2e_1^2} - \frac{hz^2\epsilon^2Z_P{}^2}{2\delta^2\nu^2e_1^2} \\ &- \frac{hz^2\epsilon^2\,\mathrm{Coth}\left(\frac{h\delta}{D_n}\right)\mathrm{Csch}\left(\frac{h\delta}{D_n}\right)Z_P}{\delta^2\nu^2e_1^2} \\ &+ \frac{z^3\epsilon^2\,\mathrm{Coth}\left(\frac{h\delta}{D_n}\right)\mathrm{Csch}\left(\frac{h\delta}{D_n}\right)Z_P}{3\delta^2\nu^2e_1^2} \\ &+ \frac{z^3\epsilon^2Z_P{}^2}{6\delta^2\nu^2e_1^2} + \frac{hz^2\epsilon^2\,\mathrm{Coth}\left(\frac{h\delta}{D_n}\right)^2Z_P{}^2}{2\delta^2\nu^2e_1^2} \\ &- \frac{z^3\epsilon^2\,\mathrm{Coth}\left(\frac{h\delta}{D_n}\right)^2Z_P{}^2}{6\delta^2\nu^2e_1^2}\end{aligned} \tag{A.1}$$

$$\begin{aligned}A_1 = &-\frac{z^2\epsilon^2\mathrm{Csch}\left(\frac{h\delta}{D_n}\right)}{\delta^3\nu^2e_1^2} - \frac{hz^2\epsilon^2\,\mathrm{Coth}\left(\frac{h\delta}{D_n}\right)}{2\delta^3\nu^2e_1^2H_0} \\ &+ \frac{z^3\epsilon^2\,\mathrm{Coth}\left(\frac{h\delta}{D_n}\right)}{6\delta^3\nu^2e_1^2H_0} + \frac{hz^2\epsilon^2\mathrm{Csch}\left(\frac{h\delta}{D_n}\right)}{\delta^3\nu^2e_1^2H_0} \\ &- \frac{z^3\epsilon^2\mathrm{Csch}\left(\frac{h\delta}{D_n}\right)}{6\delta^3\nu^2e_1^2H_0} + \frac{3z^2\epsilon^2\,\mathrm{Coth}\left(\frac{h\delta}{D_n}\right)Z_P}{2\delta^3\nu^2e_1^2} \\ &- \frac{z^2\epsilon^2\mathrm{Csch}\left(\frac{h\delta}{D_n}\right)Z_P}{2\delta^3\nu^2e_1^2} - \frac{hz^2\epsilon^2\,\mathrm{Coth}\left(\frac{h\delta}{D_n}\right)Z_P}{\delta^3\nu^2e_1^2H_0} \\ &+ \frac{z^3\epsilon^2\,\mathrm{Coth}\left(\frac{h\delta}{D_n}\right)Z_P}{6\delta^3\nu^2e_1^2H_0} + \frac{hz^2\epsilon^2\mathrm{Csch}\left(\frac{h\delta}{D_n}\right)Z_P}{2\delta^3\nu^2e_1^2H_0} \\ &- \frac{z^3\epsilon^2\mathrm{Csch}\left(\frac{h\delta}{D_n}\right)Z_P}{6\delta^3\nu^2e_1^2H_0} \\ &+ \frac{z^2\epsilon^2\,\mathrm{Coth}\left(\frac{h\delta}{D_n}\right)Z_P{}^2}{2\delta^3\nu^2e_1^2} - \frac{z^2\epsilon^2\mathrm{Csch}\left(\frac{h\delta}{D_n}\right)Z_P{}^2}{2\delta^3\nu^2e_1^2}\end{aligned} \tag{A.2}$$

$$A_2 = \frac{5z\epsilon^2}{\delta^4\nu^2e_1^2} + \frac{3z\epsilon^2\,\mathrm{Coth}\left(\frac{h\delta}{D_n}\right)^2}{\delta^4\nu^2e_1^2} - \frac{hz\epsilon^2}{\delta^4\nu^2e_1^2H_0} - \frac{z^2\epsilon^2\,\mathrm{Coth}\left(\frac{h\delta}{D_n}\right)\mathrm{Csch}\left(\frac{h\delta}{D_n}\right)}{2\delta^4\nu^2e_1^2H_0} + \frac{z^2\epsilon^2\mathrm{Csch}\left(\frac{h\delta}{D_n}\right)^2}{2\delta^4\nu^2e_1^2H_0} + \frac{z\epsilon^2Z_P}{\delta^4\nu^2e_1^2} - \frac{6z\epsilon^2\,\mathrm{Coth}\left(\frac{h\delta}{D_n}\right)\mathrm{Csch}\left(\frac{h\delta}{D_n}\right)Z_P}{\delta^4\nu^2e_1^2} + \frac{z^2\epsilon^2\,\mathrm{Coth}\left(\frac{h\delta}{D_n}\right)^2Z_P}{2\delta^4\nu^2e_1^2H_0} - \frac{z^2\epsilon^2\,\mathrm{Coth}\left(\frac{h\delta}{D_n}\right)\mathrm{Csch}\left(\frac{h\delta}{D_n}\right)Z_P}{\delta^4\nu^2e_1^2H_0} + \frac{z^2\epsilon^2\mathrm{Csch}\left(\frac{h\delta}{D_n}\right)^2Z_P}{2\delta^4\nu^2e_1^2H_0} + \frac{3z\epsilon^2\mathrm{Csch}\left(\frac{h\delta}{D_n}\right)^2{Z_P}^2}{\delta^4\nu^2e_1^2} + \frac{z^2\epsilon^2\,\mathrm{Coth}\left(\frac{h\delta}{D_n}\right)^2{Z_P}^2}{2\delta^4\nu^2e_1^2H_0} - \frac{z^2\epsilon^2\,\mathrm{Coth}\left(\frac{h\delta}{D_n}\right)\mathrm{Csch}\left(\frac{h\delta}{D_n}\right){Z_P}^2}{2\delta^4\nu^2e_1^2H_0} \tag{A.3}$$

$$A_3 = -\frac{3\epsilon^2\,\mathrm{Coth}\left(\frac{h\delta}{D_n}\right)}{\delta^5\nu^2e_1^2} + \frac{2\epsilon^2\,\mathrm{Cosh}\left(\frac{(h-z)\delta}{D_n}\right)\mathrm{Csch}\left(\frac{h\delta}{D_n}\right)}{\delta^5\nu^2e_1^2} + \frac{\epsilon^2\mathrm{Csch}\left(\frac{h\delta}{D_n}\right)\mathrm{Sinh}\left(\frac{(h-z)\delta}{D_n}\right)}{\delta^5\nu^2e_1^2} + \frac{\epsilon^2\,\mathrm{Coth}(\frac{h\delta}{D_N})\mathrm{Csch}\left(\frac{h\delta}{D_n}\right)\mathrm{Sinh}\left(\frac{(h-z)\delta}{D_n}\right)}{\delta^5\nu^2e_1^2} + \frac{h\epsilon^2\,\mathrm{Coth}\left(\frac{h\delta}{D_n}\right)}{\delta^5\nu^2e_1^2H_0} + \frac{z\epsilon^2\,\mathrm{Coth}\left(\frac{h\delta}{D_n}\right)}{\delta^5\nu^2e_1^2H_0} - \frac{z\epsilon^2\mathrm{Csch}\left(\frac{h\delta}{D_n}\right)}{\delta^5\nu^2e_1^2H_0} - \frac{h\epsilon^2\,\mathrm{Cosh}\left(\frac{(h-z)\delta}{D_n}\right)\mathrm{Csch}\left(\frac{h\delta}{D_n}\right)}{\delta^5\nu^2e_1^2H_0} - \frac{\epsilon^2\,\mathrm{Coth}\left(\frac{h\delta}{D_n}\right)Z_P}{\delta^5\nu^2e_1^2} + \frac{3\epsilon^2\mathrm{Csch}\left(\frac{h\delta}{D_n}\right)Z_P}{\delta^5\nu^2e_1^2} + \frac{\epsilon^2\,\mathrm{Cosh}\left(\frac{(h-z)\delta}{D_n}\right)\mathrm{Csch}\left(\frac{h\delta}{D_n}\right)Z_P}{\delta^5\nu^2e_1^2} - \frac{2\epsilon^2\,\mathrm{Cosh}\left(\frac{z\delta}{D_n}\right)\mathrm{Csch}\left(\frac{h\delta}{D_n}\right)Z_P}{\delta^5\nu^2e_1^2} - \frac{\epsilon^2\mathrm{Csch}\left(\frac{h\delta}{D_n}\right)^2\mathrm{Sinh}\left(\frac{(h-z)\delta}{D_n}\right)Z_P}{\delta^5\nu^2e_1^2} + \frac{\epsilon^2\mathrm{Csch}\left(\frac{h\delta}{D_n}\right)\mathrm{Sinh}\left(\frac{z\delta}{D_n}\right)Z_P}{\delta^5\nu^2e_1^2} + \frac{\epsilon^2\,\mathrm{Coth}\left(\frac{h\delta}{D_n}\right)\mathrm{Csch}\left(\frac{h\delta}{D_n}\right)\mathrm{Sinh}\left(\frac{z\delta}{D_n}\right)Z_P}{\delta^5\nu^2e_1^2} + \frac{z\epsilon^2\,\mathrm{Coth}\left(\frac{h\delta}{D_n}\right)Z_P}{\delta^5\nu^2e_1^2H_0} - \frac{h\epsilon^2\mathrm{Csch}\left(\frac{h\delta}{D_n}\right)Z_P}{\delta^5\nu^2e_1^2H_0} - \frac{z\epsilon^2\mathrm{Csch}\left(\frac{h\delta}{D_n}\right)Z_P}{\delta^5\nu^2e_1^2H_0} + \frac{h\epsilon^2\,\mathrm{Cosh}\left(\frac{z\delta}{D_n}\right)\mathrm{Csch}\left(\frac{h\delta}{D_n}\right)Z_P}{\delta^5\nu^2e_1^2H_0} + \frac{\epsilon^2\mathrm{Csch}\left(\frac{h\delta}{D_n}\right)Z_P{}^2}{\delta^5\nu^2e_1^2} - \frac{\epsilon^2\,\mathrm{Cosh}\left(\frac{z\delta}{D_n}\right)\mathrm{Csch}\left(\frac{h\delta}{D_n}\right)Z_P{}^2}{\delta^5\nu^2e_1^2} - \frac{\epsilon^2\mathrm{Csch}\left(\frac{h\delta}{D_n}\right)^2\mathrm{Sinh}\left(\frac{z\delta}{D_n}\right)Z_P{}^2}{\delta^5\nu^2e_1^2} - \frac{\epsilon^2}{\delta^5\nu^2e_1^2} \tag{A.4}$$

$$A_4 = -\frac{\epsilon^2\,\mathrm{Coth}\left(\frac{h\delta}{D_n}\right)^2}{\delta^6\nu^2e_1^2H_0} + \frac{\epsilon^2\,\mathrm{Coth}\left(\frac{h\delta}{D_n}\right)\mathrm{Csch}\left(\frac{h\delta}{D_n}\right)}{\delta^6\nu^2e_1^2H_0} + \frac{\epsilon^2\,\mathrm{Cosh}\left(\frac{(h-z)\delta}{D_n}\right)\mathrm{Coth}\left(\frac{h\delta}{D_n}\right)\mathrm{Csch}\left(\frac{h\delta}{D_n}\right)}{\delta^6\nu^2e_1^2H_0} - \frac{\epsilon^2\,\mathrm{Cosh}\left(\frac{(h-z)\delta}{D_n}\right)\mathrm{Csch}\left(\frac{h\delta}{D_n}\right)^2}{\delta^6\nu^2e_1^2H_0} - \frac{\epsilon^2\,\mathrm{Coth}\left(\frac{h\delta}{D_n}\right)^2Z_P}{\delta^6\nu^2e_1^2H_0} + \frac{2\epsilon^2\,\mathrm{Coth}\left(\frac{h\delta}{D_n}\right)\mathrm{Csch}\left(\frac{h\delta}{D_n}\right)Z_P}{\delta^6\nu^2e_1^2H_0} + \frac{\epsilon^2\,\mathrm{Cosh}\left(\frac{(h-z)\delta}{D_n}\right)\mathrm{Coth}\left(\frac{h\delta}{D_n}\right)\mathrm{Csch}\left(\frac{h\delta}{D_n}\right)Z_P}{\delta^6\nu^2e_1^2H_0} - \frac{\epsilon^2\,\mathrm{Cosh}\left(\frac{z\delta}{D_n}\right)\mathrm{Coth}\left(\frac{h\delta}{D_n}\right)\mathrm{Csch}\left(\frac{h\delta}{D_n}\right)Z_P}{\delta^6\nu^2e_1^2H_0} - \frac{\epsilon^2\mathrm{Csch}\left(\frac{h\delta}{D_n}\right)^2Z_P}{\delta^6\nu^2e_1^2H_0} - \frac{\epsilon^2\,\mathrm{Cosh}\left(\frac{(h-z)\delta}{D_n}\right)\mathrm{Csch}\left(\frac{h\delta}{D_n}\right)^2Z_P}{\delta^6\nu^2e_1^2H_0} + \frac{\epsilon^2\,\mathrm{Cosh}\left(\frac{z\delta}{D_n}\right)\mathrm{Csch}\left(\frac{h\delta}{D_n}\right)^2Z_P}{\delta^6\nu^2e_1^2H_0} + \frac{\epsilon^2\,\mathrm{Coth}\left(\frac{h\delta}{D_n}\right)\mathrm{Csch}\left(\frac{h\delta}{D_n}\right)Z_P{}^2}{\delta^6\nu^2e_1^2H_0} - \frac{\epsilon^2\,\mathrm{Cosh}\left(\frac{z\delta}{D_n}\right)\mathrm{Coth}\left(\frac{h\delta}{D_n}\right)\mathrm{Csch}\left(\frac{h\delta}{D_n}\right)Z_P{}^2}{\delta^6\nu^2e_1^2H_0} - \frac{\epsilon^2\mathrm{Csch}\left(\frac{h\delta}{D_n}\right)^2Z_P{}^2}{\delta^6\nu^2e_1^2H_0} + \frac{\epsilon^2\,\mathrm{Cosh}\left(\frac{z\delta}{D_n}\right)\mathrm{Csch}\left(\frac{h\delta}{D_n}\right)^2Z_P{}^2}{\delta^6\nu^2e_1^2H_0} \tag{A.5}$$

and coefficients of the terms in the expansion of c_1 are

$$B_0 = \frac{h^3\epsilon^2 \mathrm{Csch}\left(\frac{h\delta}{D_n}\right)^2}{3\delta^2\nu^3 H_0 e_1^2} + \frac{h^4\epsilon^2}{3\delta^2\nu^3 e_1^2 {H_0}^2} - \frac{2}{3\nu}h^3k^2\gamma\delta^3 + \frac{h^2\epsilon}{2e_1\nu e_2} - \frac{5h^3\epsilon^2 Z_P}{6\delta^2\nu^3 H_0 e_1^2} - \frac{2h^3\epsilon^2 \mathrm{Coth}\left(\frac{h\delta}{D_n}\right)\mathrm{Csch}\left(\frac{h\delta}{D_n}\right)Z_P}{3\delta^2\nu^3 H_0 e_1^2} - \frac{h^3\epsilon^2 {Z_P}^2}{3\delta^2\nu^3 H_0 e_1^2} + \frac{h^3\epsilon^2 \mathrm{Coth}\left(\frac{h\delta}{D_n}\right)^2 {Z_P}^2}{3\delta^2\nu^3 H_0 e_1^2} \quad (A.6)$$

$$B_1 = -\frac{h^2\epsilon^2 \mathrm{Csch}\left(\frac{h\delta}{D_n}\right)}{\delta^3\ \ \nu^3\ \ H_0 e_1^2} - \frac{h^3\epsilon^2 \mathrm{Coth}\left(\frac{h\delta}{D_n}\right)}{3\delta^3\ \ \nu^3 e_1^2 {H_0}^2} + \frac{5h^3\epsilon^2 \mathrm{Csch}\left(\frac{h\delta}{D_n}\right)}{6\delta^3\ \ \nu^3 e_1^2 {H_0}^2} + \frac{3h^2\epsilon^2 \mathrm{Coth}\left(\frac{h\delta}{D_n}\right)Z_P}{2\delta^3\ \ \nu^3\ \ H_0 e_1^2} - \frac{h^2\epsilon^2 \mathrm{Csch}\left(\frac{h\delta}{D_n}\right)Z_P}{2\delta^3\ \ \nu^3\ \ H_0 e_1^2} - \frac{5h^3\epsilon^2 \mathrm{Coth}\left(\frac{h\delta}{D_n}\right)Z_P}{6\delta^3\ \ \nu^3 e_1^2 {H_0}^2} + \frac{h^3\epsilon^2 \mathrm{Csch}\left(\frac{h\delta}{D_n}\right)Z_P}{3\delta^3\ \ \nu^3 e_1^2 {H_0}^2} + \frac{h^2\epsilon^2 \mathrm{Coth}\left(\frac{h\delta}{D_n}\right){Z_P}^2}{2\delta^3\ \ \nu^3 H_0 e_1^2} - \frac{h^2\epsilon^2 \mathrm{Csch}\left(\frac{h\delta}{D_n}\right){Z_P}^2}{2\delta^3\ \ \nu^3\ \ H_0 e_1^2} \quad (A.7)$$

$$B_2 = \frac{5h\epsilon^2}{\delta^4\ \ \nu^3\ \ H_0 e_1^2} + \frac{3h\epsilon^2 \mathrm{Coth}\left(\frac{h\delta}{D_n}\right)^2}{\delta^4\ \ \nu^3 H_0 e_1^2} - \frac{h^2\epsilon^2}{\delta^4\ \ \nu^3 e_1^2 {H_0}^2} - \frac{h^2\epsilon^2 \mathrm{Coth}\left(\frac{h\delta}{D_n}\right)\mathrm{Csch}\left(\frac{h\delta}{D_n}\right)}{2\delta^4\ \ \nu^3 e_1^2 {H_0}^2} + \frac{h^2\epsilon^2 \mathrm{Csch}\left(\frac{h\delta}{D_n}\right)^2}{2\delta^4\ \ \nu^3 e_1^2 {H_0}^2} + \frac{h\epsilon^2 Z_P}{\delta^4\ \ \nu^3\ \ H_0 e_1^2} - \frac{6h\epsilon^2 \mathrm{Coth}\left(\frac{h\delta}{D_n}\right)\mathrm{Csch}\left(\frac{h\delta}{D_n}\right)Z_P}{\delta^4\ \ \nu^3\ \ H_0 e_1^2} + \frac{h^2\epsilon^2 \mathrm{Coth}\left(\frac{h\delta}{D_n}\right)^2 Z_P}{2\delta^4\ \ \nu^3 e_1^2 {H_0}^2} - \frac{h^2\epsilon^2 \mathrm{Coth}\left(\frac{h\delta}{D_n}\right)\mathrm{Csch}\left(\frac{h\delta}{D_n}\right)Z_P}{\delta^4\ \ \nu^3 e_1^2 {H_0}^2} + \frac{h^2\epsilon^2 \mathrm{Csch}\left(\frac{h\delta}{D_n}\right)^2 Z_P}{2\delta^4\ \ \nu^3 e_1^2 {H_0}^2} + \frac{3h\epsilon^2 \mathrm{Csch}\left(\frac{h\delta}{D_n}\right)^2 {Z_P}^2}{\delta^4\ \ \nu^3\ \ H_0 e_1^2} + \frac{h^2\epsilon^2 \mathrm{Coth}\left(\frac{h\delta}{D_n}\right)^2 {Z_P}^2}{2\delta^4\ \ \nu^3 e_1^2 {H_0}^2} - \frac{h^2\epsilon^2 \mathrm{Coth}\left(\frac{h\delta}{D_n}\right)\mathrm{Csch}\left(\frac{h\delta}{D_n}\right){Z_P}^2}{2\delta^4\ \ \nu^3 e_1^2 {H_0}^2} \quad (A.8)$$

$$B_3 = -\frac{\epsilon^2}{\delta^5\nu^3 H_0 e_1^2} - \frac{3\epsilon^2 \mathrm{Coth}\left(\frac{h\delta}{D_n}\right)}{\delta^5\nu^3 H_0 e_1^2} + \frac{2\epsilon^2 \mathrm{Csch}\left(\frac{h\delta}{D_n}\right)}{\delta^5\nu^3 H_0 e_1^2} + \frac{2h\epsilon^2 \mathrm{Coth}\left(\frac{h\delta}{D_n}\right)}{\delta^5\nu^3 e_1^2 {H_0}^2} - \frac{2h\epsilon^2 \mathrm{Csch}\left(\frac{h\delta}{D_n}\right)}{\delta^5\nu^3 e_1^2 {H_0}^2} + \frac{\epsilon^2 Z_P}{\delta^5\nu^3 H_0 e_1^2} - \frac{2\epsilon^2 \mathrm{Coth}\left(\frac{h\delta}{D_n}\right)Z_P}{\delta^5\nu^3 H_0 e_1^2} + \frac{4\epsilon^2 \mathrm{Csch}\left(\frac{h\delta}{D_n}\right)Z_P}{\delta^5\nu^3 H_0 e_1^2} + \frac{2h\epsilon^2 \mathrm{Coth}\left(\frac{h\delta}{D_n}\right)Z_P}{\delta^5\nu^3 e_1^2 {H_0}^2} - \frac{2h\epsilon^2 \mathrm{Csch}\left(\frac{h\delta}{D_n}\right)Z_P}{\delta^5\nu^3 e_1^2 {H_0}^2} - \frac{\epsilon^2 \mathrm{Coth}\left(\frac{h\delta}{D_n}\right){Z_P}^2}{\delta^5\nu^3 H_0 e_1^2} \quad (A.9)$$

$$B_4 = -\frac{\epsilon^2 \mathrm{Coth}\left(\frac{h\delta}{D_n}\right)^2}{\delta^6\ \ \nu^3 e_1^2 {H_0}^2} + \frac{2\epsilon^2 \mathrm{Coth}\left(\frac{h\delta}{D_n}\right)\mathrm{Csch}\left(\frac{h\delta}{D_n}\right)}{\delta^6\ \ \nu^3 e_1^2 {H_0}^2} - \frac{\epsilon^2 \mathrm{Csch}\left(\frac{h\delta}{D_n}\right)^2}{\delta^6\ \ \nu^3 e_1^2 {H_0}^2} - \frac{2\epsilon^2 \mathrm{Coth}\left(\frac{h\delta}{D_n}\right)^2 Z_P}{\delta^6\nu^3 e_1^2 {H_0}^2} + \frac{4\epsilon^2 \mathrm{Coth}\left(\frac{h\delta}{D_n}\right)\mathrm{Csch}\left(\frac{h\delta}{D_n}\right)Z_P}{\delta^6\ \ \nu^3 e_1^2 {H_0}^2} - \frac{2\epsilon^2 \mathrm{Csch}\left(\frac{h\delta}{D_n}\right)^2 Z_P}{\delta^6\ \ \nu^3 e_1^2 {H_0}^2} - \frac{\epsilon^2 \mathrm{Coth}\left(\frac{h\delta}{D_n}\right)^2 {Z_P}^2}{\delta^6\ \ \nu^3 e_1^2 {H_0}^2} + \frac{2\epsilon^2 \mathrm{Coth}\left(\frac{h\delta}{D_n}\right)\mathrm{Csch}\left(\frac{h\delta}{D_n}\right){Z_P}^2}{\delta^6\ \ \nu^3 e_1^2 {H_0}^2} - \frac{\epsilon^2 \mathrm{Csch}\left(\frac{h\delta}{D_n}\right)^2 {Z_P}^2}{\delta^6\ \ \nu^3 e_1^2 {H_0}^2} \quad (A.10)$$

Appendix B

The solution of the growth rate function gives the following coefficients in the expansion of G

$$F_0 = \frac{h^3k^2\epsilon^2 \mathrm{Csch}\left(\frac{h\delta}{D_n}\right)^2}{3\delta^2\nu^3 H_0 e_1^2} + \frac{h^4k^2\epsilon^2}{3\delta^2\nu^3 e_1^2 {H_0}^2} - \frac{2}{3\nu}h^3k^4\gamma\delta^3 + \frac{h^2k^2\epsilon}{2e_1\nu e_2} - \frac{5h^3k^2\epsilon^2 Z_P}{6\delta^2\nu^3 H_0 e_1^2} - \frac{2h^3k^2\epsilon^2 \mathrm{Coth}\left(\frac{h\delta}{D_n}\right)\mathrm{Csch}\left(\frac{h\delta}{D_n}\right)Z_P}{3\delta^2\nu^3 H_0 e_1^2} - \frac{h^3k^2\epsilon^2 {Z_P}^2}{3\delta^2\nu^3 H_0 e_1^2} + \frac{h^3k^2\epsilon^2 \mathrm{Coth}\left(\frac{h\delta}{D_n}\right)^2 {Z_P}^2}{3\delta^2\nu^3 H_0 e_1^2} \quad (B.1)$$

$$F_1 = -\frac{h^2k^2\epsilon^2\mathrm{Csch}\left(\frac{h\delta}{D_n}\right)}{\delta^3\ \nu^3\ H_0e_1^2} - \frac{h^3k^2\epsilon^2\,\mathrm{Coth}\left(\frac{h\delta}{D_n}\right)}{3\delta^3\ \nu^3e_1^2H_0{}^2} + \frac{5h^3k^2\epsilon^2\mathrm{Csch}\left(\frac{h\delta}{D_n}\right)}{6\delta^3\ \nu^3e_1^2H_0{}^2} - \frac{h^2k^2\epsilon^2\mathrm{Csch}\left(\frac{h\delta}{D_n}\right)Z_P}{2\delta^3\ \nu^3\ H_0e_1^2} - \frac{5h^3k^2\epsilon^2\,\mathrm{Coth}\left(\frac{h\delta}{D_n}\right)Z_P}{6\delta^3\ \nu^3e_1^2H_0{}^2} + \frac{h^3k^2\epsilon^2\mathrm{Csch}\left(\frac{h\delta}{D_n}\right)Z_P}{3\delta^3\ \nu^3e_1^2H_0{}^2} + \frac{h^2k^2\epsilon^2\,\mathrm{Coth}\left(\frac{h\delta}{D_n}\right)Z_P{}^2}{2\delta^3\ \nu^3H_0e_1^2} - \frac{h^2k^2\epsilon^2\mathrm{Csch}\left(\frac{h\delta}{D_n}\right)Z_P{}^2}{2\delta^3\ \nu^3\ H_0e_1^2} + \frac{3h^2k^2\epsilon^2\,\mathrm{Coth}\left(\frac{h\delta}{D_n}\right)Z_P}{2\delta^3\ \nu^3\ H_0e_1^2} \tag{B.2}$$

$$F_2 = \frac{5hk^2\epsilon^2}{\delta^4\ \nu^3\ H_0e_1^2} + \frac{3hk^2\epsilon^2\,\mathrm{Coth}\left(\frac{h\delta}{D_n}\right)^2}{\delta^4\ \nu^3H_0e_1^2} - \frac{h^2k^2\epsilon^2}{\delta^4\ \nu^3e_1^2H_0{}^2} - \frac{h^2k^2\epsilon^2\,\mathrm{Coth}\left(\frac{h\delta}{D_n}\right)\mathrm{Csch}\left(\frac{h\delta}{D_n}\right)}{2\delta^4\ \nu^3e_1^2H_0{}^2} + \frac{h^2k^2\epsilon^2\mathrm{Csch}\left(\frac{h\delta}{D_n}\right)^2}{2\delta^4\ \nu^3e_1^2H_0{}^2} + \frac{hk^2\epsilon^2Z_P}{\delta^4\ \nu^3\ H_0e_1^2} - \frac{6hk^2\epsilon^2\,\mathrm{Coth}\left(\frac{h\delta}{D_n}\right)\mathrm{Csch}\left(\frac{h\delta}{D_n}\right)Z_P}{\delta^4\ \nu^3\ H_0e_1^2} + \frac{h^2k^2\epsilon^2\,\mathrm{Coth}\left(\frac{h\delta}{D_n}\right)^2Z_P}{2\delta^4\ \nu^3e_1^2H_0{}^2} - \frac{h^2k^2\epsilon^2\,\mathrm{Coth}\left(\frac{h\delta}{D_n}\right)\mathrm{Csch}\left(\frac{h\delta}{D_n}\right)Z_P}{\delta^4\ \nu^3e_1^2H_0{}^2} + \frac{h^2k^2\epsilon^2\mathrm{Csch}\left(\frac{h\delta}{D_n}\right)^2Z_P}{2\delta^4\ \nu^3e_1^2H_0{}^2} + \frac{3hk^2\epsilon^2\mathrm{Csch}\left(\frac{h\delta}{D_n}\right)^2Z_P{}^2}{\delta^4\ \nu^3\ H_0e_1^2} + \frac{h^2k^2\epsilon^2\,\mathrm{Coth}\left(\frac{h\delta}{D_n}\right)^2Z_P{}^2}{2\delta^4\ \nu^3e_1^2H_0{}^2} - \frac{h^2k^2\epsilon^2\,\mathrm{Coth}\left(\frac{h\delta}{D_n}\right)\mathrm{Csch}\left(\frac{h\delta}{D_n}\right)Z_P{}^2}{2\delta^4\ \nu^3e_1^2H_0{}^2} \tag{B.3}$$

$$F_3 = -\frac{k^2\epsilon^2}{\delta^5\nu^3H_0e_1^2} - \frac{3k^2\epsilon^2\,\mathrm{Coth}\left(\frac{h\delta}{D_n}\right)}{\delta^5\nu^3H_0e_1^2} + \frac{2k^2\epsilon^2\mathrm{Csch}\left(\frac{h\delta}{D_n}\right)}{\delta^5\nu^3H_0e_1^2} + \frac{2hk^2\epsilon^2\,\mathrm{Coth}\left(\frac{h\delta}{D_n}\right)}{\delta^5\nu^3e_1^2H_0{}^2} - \frac{2hk^2\epsilon^2\mathrm{Csch}\left(\frac{h\delta}{D_n}\right)}{\delta^5\nu^3e_1^2H_0{}^2} + \frac{k^2\epsilon^2Z_P}{\delta^5\nu^3H_0e_1^2} - \frac{2k^2\epsilon^2\,\mathrm{Coth}\left(\frac{h\delta}{D_n}\right)Z_P}{\delta^5\nu^3H_0e_1^2} + \frac{4k^2\epsilon^2\mathrm{Csch}\left(\frac{h\delta}{D_n}\right)Z_P}{\delta^5\nu^3H_0e_1^2} + \frac{2hk^2\epsilon^2\,\mathrm{Coth}\left(\frac{h\delta}{D_n}\right)Z_P}{\delta^5\nu^3e_1^2H_0{}^2} - \frac{2hk^2\epsilon^2\mathrm{Csch}\left(\frac{h\delta}{D_n}\right)Z_P}{\delta^5\nu^3e_1^2H_0{}^2} - \frac{\epsilon^2k^2\,\mathrm{Coth}\left(\frac{h\delta}{D_n}\right)Z_P{}^2}{\delta^5\nu^3H_0e_1^2} \tag{B.4}$$

$$F_4 = -\frac{k^2\epsilon^2\,\mathrm{Coth}\left(\frac{h\delta}{D_n}\right)^2}{\delta^6\ \nu^3e_1^2H_0{}^2} + \frac{2k^2\epsilon^2\,\mathrm{Coth}\left(\frac{h\delta}{D_n}\right)\mathrm{Csch}\left(\frac{h\delta}{D_n}\right)}{\delta^6\ \nu^3e_1^2H_0{}^2} - \frac{k^2\epsilon^2\mathrm{Csch}\left(\frac{h\delta}{D_n}\right)^2}{\delta^6\ \nu^3e_1^2H_0{}^2} + \frac{4k^2\epsilon^2\,\mathrm{Coth}\left(\frac{h\delta}{D_n}\right)\mathrm{Csch}\left(\frac{h\delta}{D_n}\right)Z_P}{\delta^6\ \nu^3e_1^2H_0{}^2} - \frac{2k^2\epsilon^2\mathrm{Csch}\left(\frac{h\delta}{D_n}\right)^2Z_P}{\delta^6\ \nu^3e_1^2H_0{}^2} - \frac{\epsilon^2k^2\,\mathrm{Coth}\left(\frac{h\delta}{D_n}\right)^2Z_P{}^2}{\delta^6\ \nu^3e_1^2H_0{}^2} + \frac{2k^2\epsilon^2\,\mathrm{Coth}\left(\frac{h\delta}{D_n}\right)\mathrm{Csch}\left(\frac{h\delta}{D_n}\right)Z_P{}^2}{\delta^6\ \nu^3e_1^2H_0{}^2} - \frac{k^2\epsilon^2\mathrm{Csch}\left(\frac{h\delta}{D_n}\right)^2Z_P{}^2}{\delta^6\ \nu^3e_1^2H_0{}^2} - \frac{2k^2\epsilon^2\,\mathrm{Coth}\left(\frac{h\delta}{D_n}\right)^2Z_P}{\delta^6\nu^3e_1^2H_0{}^2}. \tag{B.5}$$

ORCID iDs

A M Morad https://orcid.org/0000-0001-7493-1201

References

[1] Thiele U 2011 On the depinning of a drop of partially wetting liquid on a rotating cylinder *J. Fluid Mech.* **671** 121–36

[2] Leslie G A, Wilson S K and Duffy B R 2011 Non-isothermal flow of a thin film of fluid with temperature-dependent viscosity on a stationary horizontal cylinder *Phys. Fluids* **23** 062101

[3] Seiden G and Thomas P J 2011 Complexity, segregation, and pattern formation in rotating-drum flows *Rev. Mod. Phys.* **83** 1323–65

[4] Leslie G A, Wilson S K and Duffy B R 2012 Thermoviscous coating and rimming flow *Q. J. Mech. Appl. Maths.* **65** 483–511

[5] Leslie G A, Wilson S K and Duffy B R 2013 Three-dimensional coating and rimming flow: a ring of fluid on a rotating horizontal cylinder *J. Fluid Mech.* **716** 51–82

[6] Morad A M and Zhukov M Y 2015 The motion of a thin liquid layer on the outer surface of a rotating cylinder *Eur. Phys. J. Plus* **130**

[7] Nazaripoor H, Koch C R and Sadrzadeh M 2017 Enhanced electrically induced micropatterning of confined thin liquid films *J. Ind. Eng. Chem. Res.* **56** 10678–88

[8] Sirwah M A and Zakaria K 2013 Nonlinear evolution of the travelling waves at the surface of a thin viscoelastic falling film *Appl. Math. Modelling* **37** 1723–52

[9] Shiryaeva E V, Vladimirov V A and Zhukov M Y 2009 Theory of rotating electrohydrodynamic flows in a liquid film *Phys. Rev.* E **80** 041603

[10] Abourabia A M, Hassan K M and Morad A M 2009 Analytical solutions of the magma equations for molten rocks in a granular matrix *Chaos Solitons Fractals* **42** 1170–80

[11] Takagi D 2010 Spreading of viscous fluids and granular materials on slopes *PhD Thesis* (Cambridge: University of Cambridge) (https://doi.org/10.17863/CAM.16098)

[12] Takagi D and Huppert H E 2010 Flow and instability of thin films on a cylinder and sphere *J. Fluid Mech.* **647** 221–38

[13] Shirsavar R, Amjadi A, Ejtehadi M, Mozaffari M and Feiz M 2012 Rotational regimes of freely suspended liquid crystal films under electric current in presence of an external electric field *Microfluid. Nanofluid.* **13** 83

[14] Amjadi A, Feiz M S and Namin R M 2015 Liquid soap film generates electricity: a suspended liquid film rotating in an external electric field as an electric generator *Microfluid. Nanofluid.* **18** 141
[15] Nasiri M, Shirsavar R, Saghaei T and Ramos A 2015 Simulation of liquid film motor: a charge induction mechanism *Microfluid. Nanofluid.* **19** 133–39
[16] Feiz M S, Namin R M and Amjadi A 2015 Theory of the liquid film motor *Phys. Rev.* E **92** 033002
[17] Sadiq I M R and Joo S W 2009 Weakly nonlinear stability snalysis of an electro-osmotic thin film free surface flow *Micrograv. Sci. Tech.* **21** S331–43
[18] Mayur M, Amiroudine S and Lasseux D 2012 Free-surface instability in electro-osmotic flows of ultrathin liquid films *Phys. Rev.* E **85** 046301
[19] Ray B, Bandyopadhyay D, Sharma A, Joo S W, Qian S and Biswas G 2013 Long-wave interfacial instabilities in a thin electrolyte film undergoing coupled electrokinetic flows: a nonlinear analysis *Microfluid. Nanofluid.* **15** 19–33
[20] Mayur M, Amiroudine S, Lasseux D and Chakraborty S 2014 Effect of interfacial Maxwell stress on time periodic electro-osmotic flow in a thin liquid film with a flat interface *Electrophoresis* **35** 670–80
[21] Kirby B J and Hasselbrink E F 2004 Zeta potential of microfluidic substrates: I. Theory, experimental techniques, and effects on separations *Electrophoresis* **25** 187–202
[22] Charwat A F, Kelly R E and Gazley C 1972 The flow and stability of thin liquid films on a rotating disk *J. Fluid Mech.* **53** 227–55
[23] Yang W, Delbende I, Fraigneau Y and Witkowski L M 2018 Axisymmetric rotating flow with free surface in a cylindrical tank Yann Fraigneau *J. Fluid Mech.* **929** 796–814
[24] Oddy M H and Santiago J G 2005 Multiple-species model for electrokinetic instability *Phys. Fluids* **17** 064108
[25] Chen C-H, Lin H, Lele S K and Santiago J G 2005 Convective and absolute electrokinetic instability with conductivity gradients *J. Fluid Mech.* **524** 263–303
[26] Storey B D, Tilley B S, Lin H and Santiago J G 2005 Electrokinetic instabilities in thin microchannels *Phys. Fluids* **17** 018103
[27] Lin H, Storey B D and Santiago J G 2008 A depth-averaged electrokinetic flow model for shallow microchannels *J. Fluid Mech.* **608** 43–70
[28] Zhang J, Song Y and Lie D 2019 Thin liquid film between a floating oil droplet and a glass slide unde dc electric field *J. Colloid Interface Sci.* **534** 262–9